# Periodic DFT study of structural transformations of crystalline

# dihydroxylammonium 5,5′-bistetrazole-1,1′-diolate under high pressures

## G.Z. Zhao[1]*, H.R. Sun[2], J.F. Jia[1], and H.S. Wu[1]

[1] School of Chemistry and Material Science, Shanxi Normal University, PR China

[2] School of Foreign Languages, Shanxi Normal University, PR China

*Presenting author: zhaoguozheng99@126.com

†Corresponding author: zhaoguozheng99@126.com

## Abstract

Density functional theory (DFT) periodic calculations were performed to study the crystal and electronic structures of energetic compound dihydroxylammonium 5,5′-bistetrazole-1,1′-diolate (TKX-50) under the pressure ranging from 0 to 400 GPa. The optimized crystal structure by the local density approximation (LDA) with CA-PZ functional matches well with the experimental values under the ambient pressure. When the structural transformations occur under the pressure of 126, 288, and 334 GPa, with the pressure increasing, the lattice constants and unit cell volume of TKX-50 change gradually. First of all, TKX-50 is rearranged in the crystal and the improvement of the molecular planarity occurs. Next, structural transformation appears with the distortion of the tetrazole rings. Finally, the rotation of molecular conformation occurs. The results of density of states show that TKX-50 crystal, with the increase of pressure, undergoes an electronic transition from the semiconductor to the metallic system. These results provide basic information for the high pressure behavior of crystalline TKX-50.

**Keywords:** density functional theory; TKX-50; high pressure; crystalline structures

## Introduction

High energetic compounds have been widely used in military and civilian applications [1–4]. To meet the continuing need for novel high energetic compounds with high explosive performance and insensitivity, many scientists have paid considerable attention to the compounds' designing and synthesizing over several decades [5−7]. Among various types of high energetic compounds, energetic ionic salts come to be a unique class of energetic compound and have received a substantial amount of interests due to their merits, such as low vapor pressures, favorable insensitivity, excellent explosive performance, and environmental acceptability [8,9].

The energetic ionic salts of azoles, which are composed of high-nitrogen cations and anions, possess a large number of energetic N=N, N–N, C=N and C–N bonds. Therefore, they exhibit high energy and positive heats of formation [10−12]. Compared with the others, the tetrazole cations or anions are more energetic owing to their higher nitrogen content [13]. Klapötke *et al.* [14], detailed the preparation of a new explosive dihydroxylammonium 5,5′-bistetrazole-1,1′-diolate (TKX-50), which is not only easily prepared and exceedingly powerful (detonation velocity 9.70 km·s⁻¹, detonation pressure 42.4GPa), but also possessing the required thermal insensitivity (decomposition onset 222℃), low toxicity, and handling safety. Luo *et al.* [15], investigated the structures, mechanical properties, and mechanical responses of TKX-50 and TKX-50 based PBX with molecular dynamics. Goddard *et al.* [16], developed a flexible classical force field for TKX-50, which reproduces the cell parameters, densities, lattice energy and mechanical properties derived from quantum mechanics (QM) and experiments.

Detailed information on the behavior of TKX-50 under high pressures is of great significance for the understanding of its chemical reactivity, detonation process, structural stabilities, and sensitivity. In the present work, the periodic DFT calculations were performed

to study the crystal structure and properties of TKX-50 under hydrostatic pressure of 0–400 GPa. Figure 1 displays crystal and molecular structures of TKX-50.
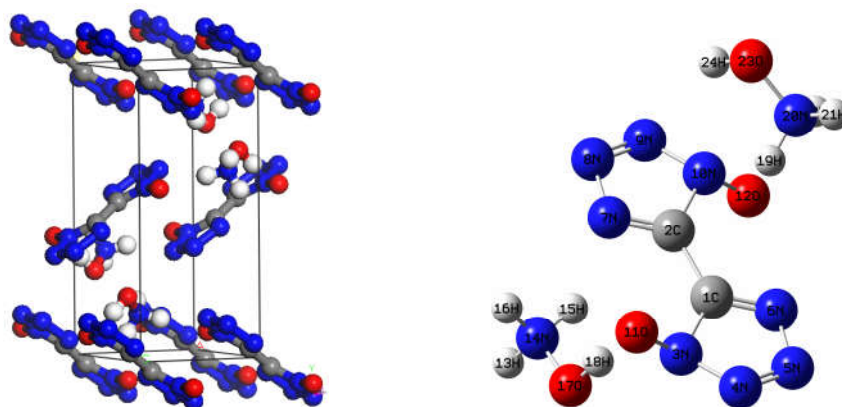


**Figure 1. Crystal and molecular structures of TKX-50**

## Computational Methods

The periodic DFT calculations were performed in combination with the Vanderbilt-type ultrasoft pseudopotential and a plane-wave expansion of the wave functions [17]. The local density approximation (LDA) with the Ceperley−Alder exchange-correlation potential parametrized by Perdew and Zunger (CA-PZ) [18,19] implemented in the CASTEP [20] module of Materials Studio 6.0 [21] were used to perform the test calculations on crystalline TKX-50. The cutoff energy of plane waves was set to 340 eV. Brillouin zones sampling was performed by using the Monkhost−Pack scheme with a $k$-point grid of $3 \times 1 \times 2$. The initial crystal was taken from Klapötke *et al*. (CCDC 872232) [14] and used for the computations.

## Results and Discussion

**Table 1. Comparison of the lattice constants of TKX-50 with experimental data at ambient conditions**

| Method | $a$ (Å) | $b$ (Å) | $c$ (Å) | Cell volume (Å$^3$) |
|---|---|---|---|---|
| LDA/CA-PZ | 5.522 (1.50) | 11.047 (-5.99) | 6.235 (-4.97) | 377.83 (-9.58) |
| GGA/PW91 | 5.061 (-6.97) | 13.171 (12.08) | 7.086 (8.00) | 468.31 (12.07) |
| GGA/PBE | 5.066 (-6.86) | 13.139 (11.81) | 7.083 (7.96) | 467.51 (11.88) |
| Exp. | 5.441 | 11.751 | 6.561 | 417.86 |

The values in parentheses correspond to the percentage differences relative to the experimental data.

Two different functionals, local density approximation (LDA) and generalized gradient approximation (GGA) were applied to the computation of crystalline TKX-50 as a test. To benchmark the performance of the theoretical approach, LDA/CA-PZ, GGA/PW91(Perdew−Wang-91) [22], and GGA/PBE (Perdew−Burke−Ernzerhof) [23] were selected to fully relax the TKX-50 at ambient pressure without any constraint. Table 1 lists the experimental and relaxed cell parameters of TKX-50 crystal. The relative errors of the calculated values to the experimental ones show that the calculated values of LDA/CA-PZ agree better with the experimental ones than those of GGA. Thus, LDA/CA-PZ method has been employed in the present study.
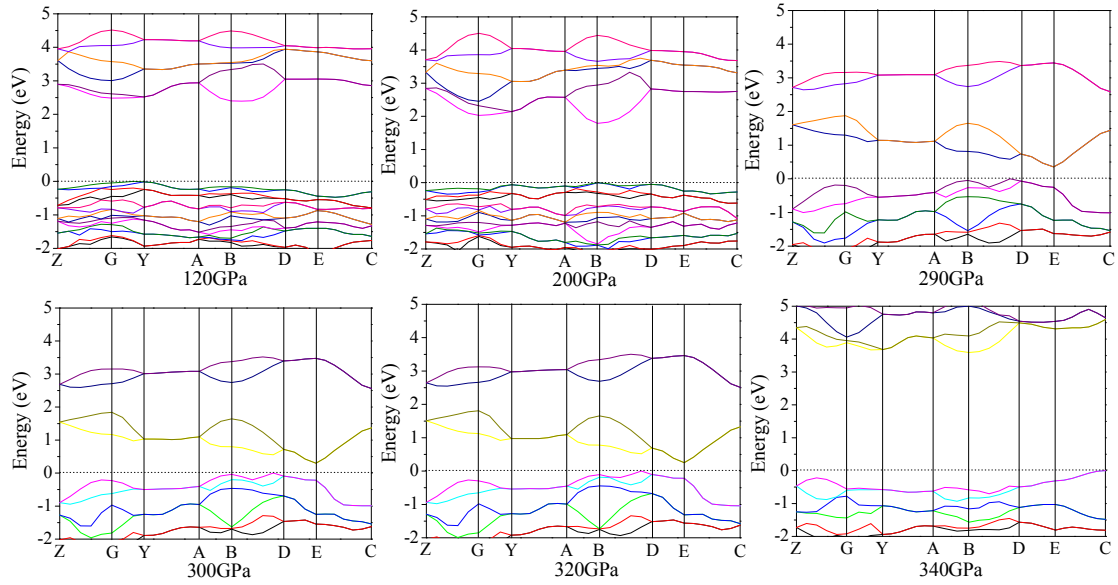
*Crystal Structure*
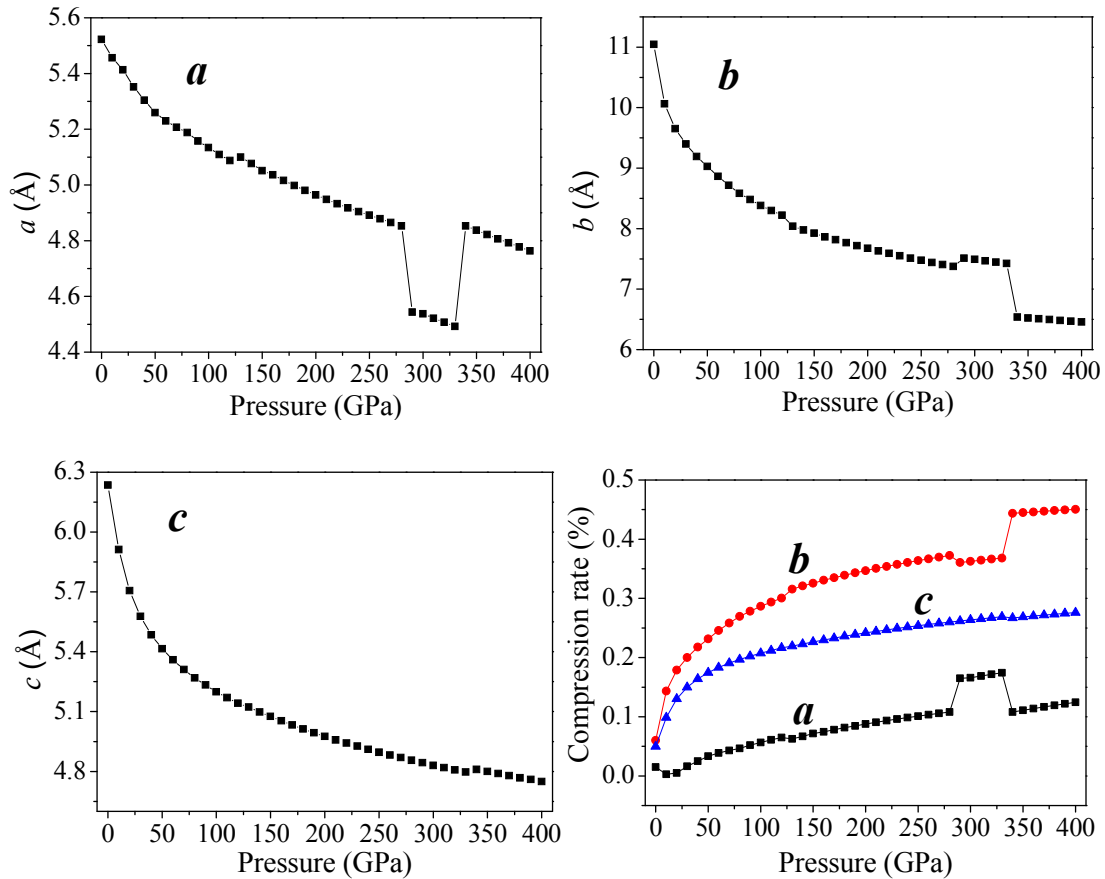
**Figure 2. Lattice constants (*a*, *b*, *c*) and compression rates of TKX-50 as a function of pressure**

The relaxed lattice constants (*a*, *b*, c) and compression rates in the pressure range of 0−400 GPa are depicted in Figure 2. With the pressure increasing, the lattice constants (*a*, *b*, *c*) and unit cell volume decrease gradually. It is because the external pressure is large enough to overcome the intermolecular repulsion along the crystallographic directions and makes the crystal structure shrink. The curves *a*, *b*, and *c* have sudden changes in magnitudes at about 126, 288, and 334 GPa, which suggest large changes have taken place. The value of *a* at 126 GPa is anomalously larger than that at 125 GPa, and increases abnormally again at 334 GPa. At 126 GPa, *b* value is much smaller than that at 125 GPa, and decreases sharply at 334 GPa. During 150−250 GPa, the lattice constants (*a*, *b*, *c*) decrease steadily, while at 334 GPa *c* increases dramatically.

The largest compression of the unit cell takes place in the pressure region below 50 GPa. With the pressure increasing from 50 to 125 GPa, and from 130 to 280 GPa, the lattice parameters decrease slowly. In the pressure range of 0−280 GPa, the compression ratios along three directions are not tantamount. At 80 GPa, the total compression ratios along the directions of *a*, *b*, and *c* are 6.9%, 28.8%, and 26.4%, respectively, which indicats that the compressibility of TKX-50 crystal is anisotropic and the structure is much stiffer in *a* direction than those in *b* and *c* directions.

*Electronic Structure*

3

**Figure 3. Self-consistent band structures of crystalline TKX-50 under different pressures. The Fermi energy is shown as a dashed horizontal line**

On the basis of the equilibrium crystal structures obtained under different pressures, the self-consistent band structures along different symmetry directions of the Brillouin zone have been calculated and are shown in Figure 3. In order to have a visualized view, there is merely a presentation of range from –2.0 to 5.0 eV. It is clear that as the pressure is raised, the energy bands of valence and conduction bands change in an obvious way. For example, if the pressure is less than 200 GPa, energy bands will be in a stable state and the intermolecular interactions are not obvious. Some important changes in the electronic properties can be got on the basis of the transformation in configuration of TKX-50 at 288 GPa. As is shown, the energy bands get to a higher energy region. That is to say, the conduction bands become wider, while the valence bands become narrower in comparision with the ones in lower pressures.
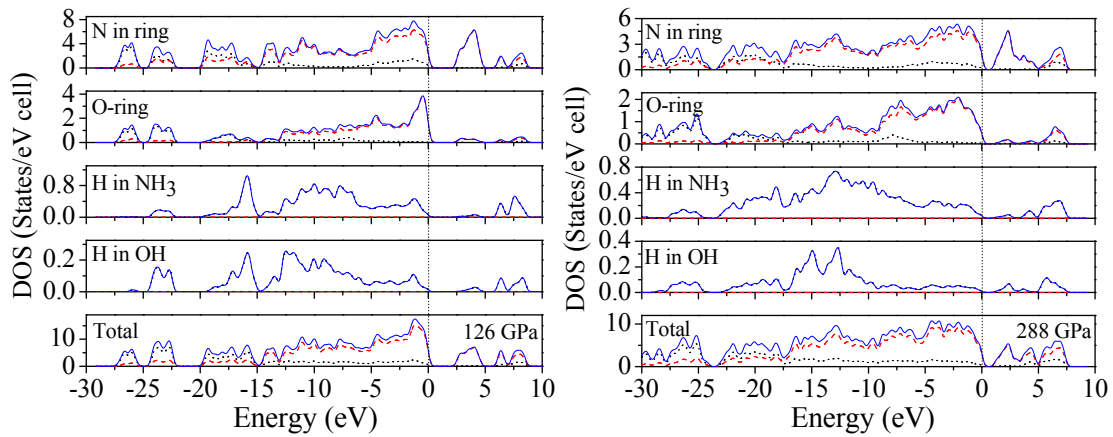


**Figure 4. The atom-resolved DOS and PDOS of TKX-50 at 126 GPa, and 288 GPa**

The atom-resolved DOS and PDOS of TKX-50 under pressure relate closely to the structural transformation. The DOS and PDOS at 126 and 288 GPa are shown in Figure 4. At 126 GPa, the upper valence bands and the lower conduction bands are predominated by the *p* states of N atoms in tetrazole rings. While at 288 GPa, the upper valence bands and the lower conduction bands are mainly contributed to the N states in tetrazole rings. Furthermore, the N states in tetrazole rings move toward the Fermi level. The structural transformations occur due to the deformation of tetrazole rings.

**Conclusions**

In this work, periodic DFT calculations have been performed to study the effect of high pressure on the crystal and electronic structures of the energetic salt TKX-50 under hydrostatic pressure of 0−400 GPa. Pressure-induced molecular structure transformations occur at 126, 288, and 334 GPa. At 126 GPa, TKX-50 molecules in crystal are rearranged, and the molecular planarity are improved by the high pressure. With the pressure increasing, the molecular structure and unit cell parameters change gradually. The second structural transformation occurs at 288 GPa with the distortion of the tetrazole rings. When the pressure reaches as high as 334 GPa, the tetrazole ring is severely distorted, and a new structure appeared with the rotation of the molecular conformation.

## Acknowledgements

## References

[1] Forquet, V., C. M. Sabate, H. Chermette, G. Jacob, E. Labarthe, H. Delalu, and C. Darwich. 2016. *Chemistry-An Asian Journal*, 11: 730−744.
[2] Tang, Y. X., C. L. He, L. A. Mitchell, D. A. Parrish, and J. M. Shreeve. 2016. *Journal of Materials Chemistry A*, 4: 3879−3885.
[3] Zhao, G. Z., and Lu M. 2017. *Journal of Energetic Materials*, 35: 63−76.
[4] Keshavarz, M. H., K. Esmaeilpour, M. Oftadeh, and Y. H. Abadi. 2015. *RSC Advances*, 5: 87392−87399.
[5] Liu, Q. Q., B. Jin, R. F. Peng, Z. C. Guo, J. Zhao, Q. C. Zhang, and Y. Shang. 2016. *Journal of Materials Chemistry A*, 4: 4971−4981.
[6] He, P. A., J. G. Zhang, K. Wang, X. Yin, and T. L. Zhang. 2015. *Journal of Organic Chemistry*, 80: 5643−5651.
[7] Myers, T. W., J. A. Bjorgaard, K. E. Brown, D. E. Chavez, S. K. Hanson, R. J. Scharff, S. Tretiak, and J. M. Veauthier. 2016. *Journal of The American Chemical Society*, 138: 4685−4692.
[8] Yin, P., C. L. He, and J. M. Shreeve. 2016. *Chemistry: A European Journal*, 22: 2108−2113.
[9] Ghosh, J., and A. Bhattacharya. 2016. *Chemical Physics*, 464: 26−39.
[10] Yin, P., D. A. Parrish, and J. M. Shreeve. 2015. *Journal of The American Chemical Society*, 137: 4778−4786.
[11] Abe, T., G. H. Tao, Y. H. Joo, R. W. Winter, G. L. Gard, and J. M. Shreeve. 2009. *Chemistry: A European Journal*, 15: 9897−9904.
[12] Klapötke, T. M., and C. M. Sabate. 2008. *European Journal of Inorganic Chemistry*, 34: 5350−5366.
[13] Fischer, D., T. M. Klapötke, and J. Stierstorfer. 2015. *Angewandte Chemie International Edition*, 54: 10299−10302.
[14] Fischer, N., D. Fischer, T. M. Klapötke, D. G. Piercey, and J. Stierstorfer. 2012. *Journal of Materials Chemistry*, 22: 20418−20422.
[15] Ma, S., Y. J. Li, Y. Li, and Y. J. Luo. 2016. *Journal of Molecular Modeling*, 22: 43.
[16] An, Q., T. Cheng, W. A. Goddard, and S. V. Zybin. 2015. *Journal of Physical Chemistry C*, 119: 2196−2207.
[17] Vanderbilt, D. 1990. *Physical Review B*, 41: 7892−7895.
[18] Ceperley, D. M., and B. J. Alder. 1980. *Physical Review Letters*, 45: 566−569.
[19] Perdew, J. P., and A. Zunger. 1981. *Physical Review B*, 23: 5048−5079.
[20] Clark, S. J., M. D. Segall, C. J. Pickard, P. J. Hasnip, M. J. Probert, K. Refson, and M. C. Payne. 2005. *Zeitschrift für Kristallographie*, 220: 567−570.
[21] Materials Studio 6.0 2012. Accelrys.
[22] Perdew, J. P., and Y. Wang. 1992. *Physical Review B*, 45: 13244−13249.
[23] Perdew, J. P., K. Burke, and M. Ernzerhof. 1996. *Physical Review Letters*, 77: 3865−3868.